Investigations into the FLG Null Phenotype: Showcasing the Methodology for CRISPR/Cas9 Editing of Human Keratinocytes

Jos P.H. Smits[1,2], Noa J.M. van den Brink[1], Luca D. Meesters[1,3], Hadia Hamdaoui[1], Hanna Niehues[1], Patrick A.M. Jansen[1], Ivonne M.J.J. van Vlijmen-Willems[1], Diana Rodijk-Olthuis[1], Céline Evrard[4], Yves Poumay[4], Michel van Geel[5,6,7], Wiljan J.A.J. Hendriks[8], Joost Schalkwijk[1], Patrick L.J.M. Zeeuwen[1] and Ellen H. van den Bogaard[1]

Ever since the association between *FLG* loss-of-function variants and ichthyosis vulgaris and atopic dermatitis disease onset was identified, FLGs function has been under investigation. Intraindividual genomic predisposition, immunological confounders, and environmental interactions complicate the comparison between *FLG* genotypes and related causal effects. Using CRISPR/Cas9, we generated human FLG-knockout (ΔFLG) N/TERT-2G keratinocytes. FLG deficiency was shown by immunohistochemistry of human epidermal equivalent cultures. Next to (partial) loss of structural proteins (involucrin, hornerin, keratin 2, and transglutaminase 1), the stratum corneum was denser and lacked the typical basket weave appearance. In addition, electrical impedance spectroscopy and transepidermal water loss analyses highlighted a compromised epidermal barrier in ΔFLG human epidermal equivalents. Correction of *FLG* reinstated the presence of keratohyalin granules in the stratum granulosum, FLG protein expression, and expression of the proteins mentioned earlier. The beneficial effects on stratum corneum formation were reflected by the normalization of electrical impedance spectroscopy and transepidermal water loss. This study shows the causal phenotypical and functional consequences of FLG deficiency, indicating that FLG is not only central in epidermal barrier function but also vital for epidermal differentiation by orchestrating the expression of other important epidermal proteins. These observations pave the way to fundamental investigations into the exact role of FLG in skin biology and disease.

Journal of Investigative Dermatology (2023) ■, ■–■; doi:10.1016/j.jid.2023.02.021

INTRODUCTION

Atopic dermatitis (AD) is a common chronic inflammatory skin condition that is characterized by itchy, dry, erythematous, plaques, and an impaired skin barrier function. The pathophysiologic basis of AD is multifactorial, including genetic polymorphisms, environmental stimuli, and deregulation of innate and adaptive immunity. The seminal work from the McLean group, identifying genetic risk factors such as loss-of-function variants in the *FLG* gene in AD (Palmer et al., 2006) and ichthyosis vulgaris (Smith et al., 2006), has caused a paradigm shift indicating that epidermal biology and the skin barrier proteins themselves are of importance in complex inflammatory skin diseases such as AD. The *FLG* gene is located at chromosome 1q21 within the epidermal differentiation complex. This gene complex encodes proteins that are typically involved in the terminal differentiation and cornification of keratinocytes (KCs). Pro-FLG protein can be proteolytically degraded into FLG monomers and further converted into natural moisturizing factors (NMFs) (Scott and Harding, 1986). Hygroscopic NMFs maintain epidermal hydration of the skin, and the reduction of NMFs directly results in dry skin (Horii et al., 1989). Loss-of-function variants in *FLG* lead to reduced levels of NMFs in the stratum corneum (Kezic et al., 2008). NMF levels directly correlate with *FLG* genotype and AD severity (Riethmuller et al., 2015) and are found to correlate with corneocyte morphology in patients with AD (Riethmuller et al., 2015). In mouse models, FLG deficiency results in barrier impairment and allergen sensitization (Kawasaki et al., 2012). When comparing patients with AD with *FLG* variants with those without, increased water loss and skin permeability were found in both groups (Flohr et al., 2010; Jakasa et al., 2011; Winge et al., 2011), whereas others report that *FLG* variants do not influence transepidermal water loss (Niehues et al., 2017). In experimental in vitro studies, the lack of consistency

[1]*Department of Dermatology, Radboud Institute for Molecular Life Sciences, Radboud University Medical Center, Nijmegen, The Netherlands;* [2]*Department of Dermatology, University Hospital Düsseldorf, Medical Faculty, Heinrich Heine University, Düsseldorf, Germany;* [3]*Department of Molecular Developmental Biology, Radboud Institute for Molecular Life Sciences, Radboud University Medical Center, Nijmegen, The Netherlands;* [4]*Molecular Physiology Research Unit, NAmur Research Institute for Life Sciences, University of Namur, Namur, Belgium;* [5]*Department of Dermatology, Maastricht University Medical Center+, Maastricht, The Netherlands;* [6]*GROW School for Oncology and Developmental Biology, Maastricht University, Maastricht, The Netherlands;* [7]*Department of Clinical Genetics, Maastricht University Medical Center+, Maastricht, The Netherlands; and* [8]*Department of Cell Biology, Radboud Institute for Molecular Life Sciences, Radboud University Medical Center, Nijmegen, The Netherlands*

Correspondence: Ellen H. van den Bogaard, Department of Dermatology, Radboud Institute for Molecular Life Sciences, Radboud University Medical Center, P. O. Box 9101, Nijmegen 6500 HB, The Netherlands. E-mail: ellen.vandenbogaard@radboudumc.nl

Abbreviations: AD, atopic dermatitis; HEE, human epidermal equivalent; HRNR, hornerin; K2, keratin 2; KC, keratinocyte; NMF, natural moisturizing factor; sgRNA, single-guide RNA

Received 23 August 2022; revised 20 January 2023; accepted 11 February 2023; accepted manuscript published online XXX; corrected proof published online XXX

between cell sources, organotypic models, and knockdown efficiencies has yielded contradictory evidence on the consequences of FLG deficiency (Niehues et al., 2017). Although the importance of FLG for healthy skin barrier development and maintenance is widely accepted, interpatient differences complicate genotype−phenotype studies, and the short life span of primary cells in culture limits the meticulous dissection of all functional properties of (pro-)FLG.

To overcome these limitations, genomic engineering by CRISPR and CRISPR/Cas9 (Cong et al., 2013; Gasiunas et al., 2012; Jinek et al., 2012; Mali et al., 2013) could be a powerful technique. Yet, the introduction of the CRISPR/Cas9 machinery into the notoriously difficult-to-transfect KCs has been proven troublesome, although many options are seemingly available (Shi et al., 2021). Some CRISPR/Cas9-related work is performed in primary KCs, although most of the published research utilizes immortalized KCs (Smits et al., 2022). The immortalized human N/TERT KC cell lines (N/TERT-1 and N/TERT-2G) have been available (Dickson et al., 2000), and our recent studies on their excellence as alternatives to primary KCs sparked great interest in these cell lines (Smits et al., 2017). N/TERT KCs are more amenable to transfection with foreign DNA or ribonucleoprotein complexes followed by clonal expansion because they are less prone to terminal differentiation than primary KCs. In addition, the N/TERT cells are diploid (Smits et al., 2017) in contrast to other immortal lines and thus very useful as an alternative to primary KCs in genome editing experiments.

In this study, we illustrate the complementary potential of both the human N/TERT KCs and a high-efficiency CRISPR/Cas9 gene-editing protocol for generating and functionally characterizing FLG-knockout (ΔFLG) isogenic N/TERT-2G KCs. The subsequent repair of the induced knockout in clonal cell lines of identical genomic background underlines the apparent genotype−phenotype relationship. These key and, to our knowledge, previously unreported aspects of pro-FLG expression and downstream regulation of epidermal biology have clear implications for our understanding of skin diseases that are characterized by the loss of FLG.

RESULTS

Generation of human ΔFLG N/TERT-2G KCs through CRISPR/Cas9

A single-guide RNA (sgRNA) was designed to target exon 3 of the *FLG* gene to disrupt FLG protein expression, as schematically visualized (Figure 1a). Immortalized human KC N/TERT-2G cells were electroporated with ribonucleoprotein complex containing the *FLG* targeting sgRNA and synthetic spCas9 protein (Evrard et al., 2021). Targeted Cas9 introduced a double strand break typically repaired through nonhomologous end joining. This efficiently generated insertions and deletions, giving rise to human ΔFLG N/TERT-2G KCs as analyzed by the Inference of CRISPR Edits webtool (http://ice.synthego.com, version 2), showing 99% insertions and deletions with 87% protein knockout prediction in the cell pool (Figure 1b). Three-dimensional human epidermal equivalents (HEEs) generated from N/TERT-2G control KCs (FLG wild-type) and the ΔFLG N/TERT-2G KC cell pool (ΔFLG pool) showed the absence of keratohyalin granules in the ΔFLG pool culture. Specific FLG protein staining validated the partial loss of FLG expression (Figure 1c). We obtained clonal cell lines by seeding single cells from the ΔFLG pool into 96-well plates, one cell per well. The ΔFLG clonal line presented (Figure 1c) was further analyzed and used throughout the study.

Characterization of *FLG* genotype−defined clonal N/TERT-2G KC cell lines

After generating a number of single-cell clones from the ΔFLG pool, we proceeded to analyze these clones for *FLG* variants at the sgRNA-targeted Cas9 cleavage site to identify which clones were likely 100% knockout for FLG protein expression. Of 14 clones isolated, 6 had mutations on both alleles but were heterozygous knockout (data not shown), whereas 3 clones were predicted and validated to be fully knockout for FLG protein expression (Supplementary Table S1 and Supplementary Figure S1). One particular ΔFLG clone showed the deletion of five bases (c.152del5) on both alleles, leading to a predicted p.P51HfsX3 frameshift mutation and an early stop codon (Figure 2a and c). This cell line was used for further experiments (ΔFLG clone).

Genomic engineering through CRISPR/Cas9 potentially introduces off-target effects. The CRISPOR tool (Concordet and Haeussler, 2018) was used to find and rank potential sgRNA-specific off-target sites on the basis of cutting frequency determination score (Supplementary Table S2). The top five potential off-target sites were amplified by PCR, and the amplicons were Sanger sequenced. None of the predicted off-target mutations were found (data not shown). In addition, to prove specific genotype−phenotype correlations, we engineered a N/TERT-2G KC cell line corrected for the five bases deletion (FLG-corrected). Hereto, a ΔFLG clone−specific sgRNA and single-strand donor oligonucleotide was designed. The single-strand donor oligonucleotide encodes the wild-type *FLG* sequence plus a silent variant (c.139-11C>T) 22 bases downstream of the protospacer adjacent motif to allow for the identification of the rescued clone from unedited wild-type cells. Through CRISPR/Cas9-induced homology-directed repair, the previously induced homozygous *FLG* variant would be restored, ultimately leading to the reinstation of FLG protein expression, as schematically depicted (Figure 2b). Homology-directed repair yielded a correction efficiency of 27%, and the FLG-corrected cell pool was expanded to generate FLG-corrected clones. Off-target effects were screened again as described earlier (Supplementary Table S3), and none were detected (data not shown).

To validate the CRISPR/Cas9-mediated genomic engineering and clonality of our cell lines, *FLG* PCR amplicons were sequenced through Sanger sequencing (Figure 2c). These results indicate the clonality of the ΔFLG clone and the FLG-corrected clone and show the introduction of the silent intronic variant in the FLG-corrected clone. The comparison of HEEs from wild-type FLG KCs (HEE^{WT}) with those from the ΔFLG clone ($HEE^{\Delta FLG}$) showed that knockout of FLG results in the absence of keratohyalin granules and abrogated FLG protein expression (Figure 2d). In the FLG-corrected clone (HEE^{COR}), the presence of keratohyalin granules was reinstated together with the complete recovery of FLG expression, as was

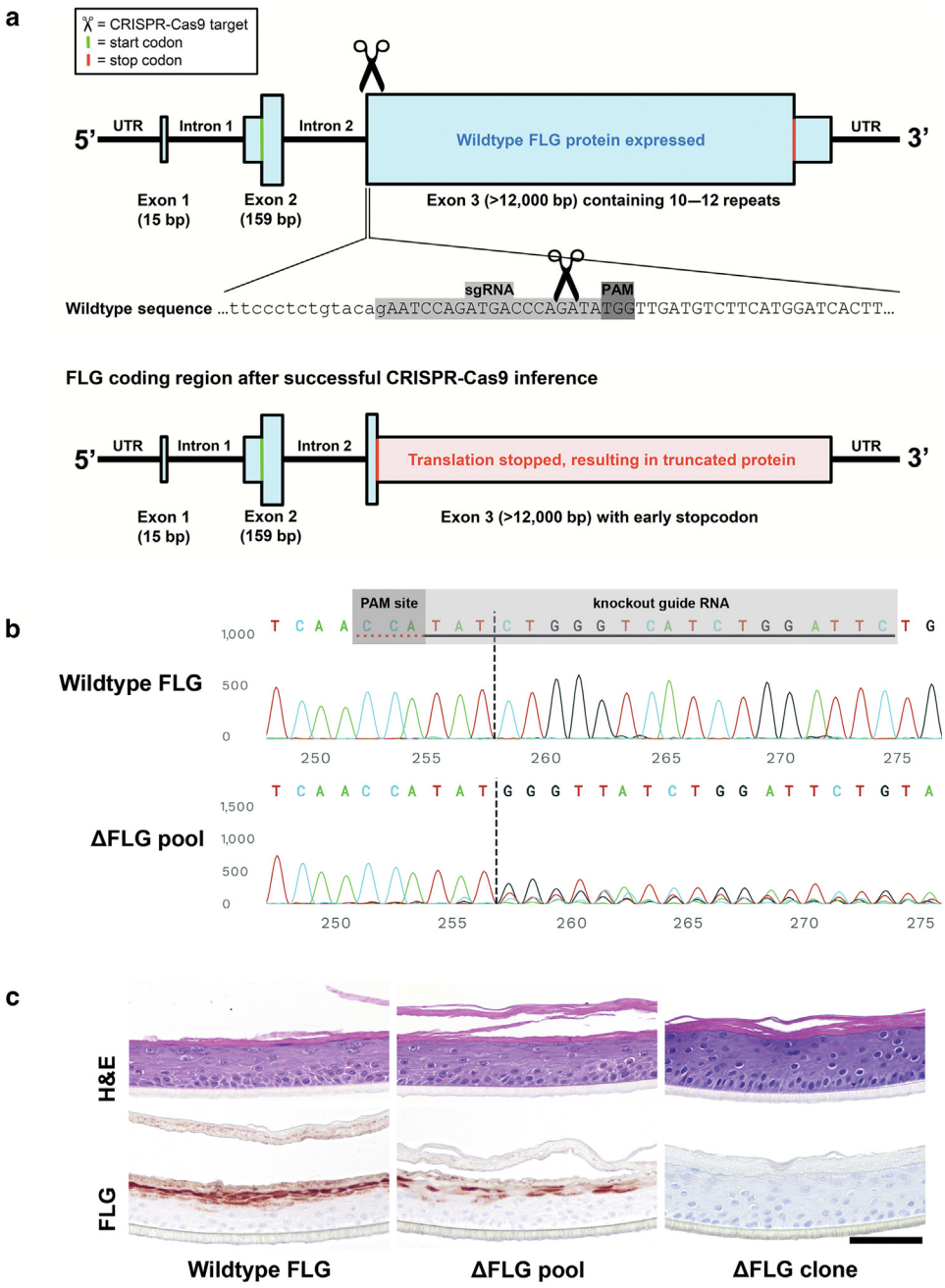

Figure 1. Generation of a ΔFLG N/TERT-2G clonal keratinocyte cell line. (**a**) Schematic representation of the FLG-knockout experiment. N/TERT-2G keratinocytes were electroporated with RNP complex containing *FLG*-specific gRNA and synthetic SpCas9 protein, introducing NHEJ-induced insertions and deletions leading to a frameshift mutation. (**b**) *FLG* gene was analyzed after PCR amplification of the knockout locus (reverse complement sequence depicted). ΔFLG pool of keratinocytes shows aberrant sequence reads starting 3 nucleotides 5′ of the PAM site. (**c**) ΔFLG pool was used to generate HEEs, showing partial loss of keratohyalin granules and FLG expression. After the clonal expansion of the ΔFLG pool, full ΔFLG clonal cells (c.152del5 encoding p.P51HfsX3) show a complete absence of keratohyalin granules and FLG protein. Bar = 100 μm. gRNA, guide RNA; HEE, human epidermal equivalent; NHEj, nonhomologous end joining; PAM, protospacer adjacent motif; RNP, ribonucleoprotein; UTR, untranslated region.

expected from the protein sequences (Supplementary Table S1).

FLG regulates epidermal differentiation gene and protein expression

Next, the expression of key epidermal marker proteins was analyzed through immunohistochemistry (Figure 3a). Interestingly, specific alterations in protein expression profiles due to the presence or absence of FLG were observed. The expression of involucrin and transglutaminase 1 was partially lost in $HEE^{\Delta FLG}$ but restored in HEE^{COR}, whereas the expression of hornerin (HRNR) and keratin 2 (K2) was completely abrogated in $HEE^{\Delta FLG}$ and (partially) restored in HEE^{COR}. The knockout of FLG expression, therefore, seems pivotal for the deregulated expression of other differentiation proteins. Keratin 10, loricrin, late cornified envelope 2, and late cornified envelope 3 were similar between HEE^{WT}, $HEE^{\Delta FLG}$, and HEE^{COR}. To assess whether the differential expression originates from transcriptional or post-translational processes, we analyzed gene expression levels corresponding to the investigated differentially expressed proteins. These gene expression levels followed a similar pattern as for protein, with strong and significantly downregulated *HRNR* and *K2* levels in the ΔFLG clone. Gene expression of *K2* was rescued upon FLG correction, although *HRNR* expression remained downregulated (Figure 3b). These results indicate that loss of FLG can lead to (sustained) transcriptional changes in KCs.

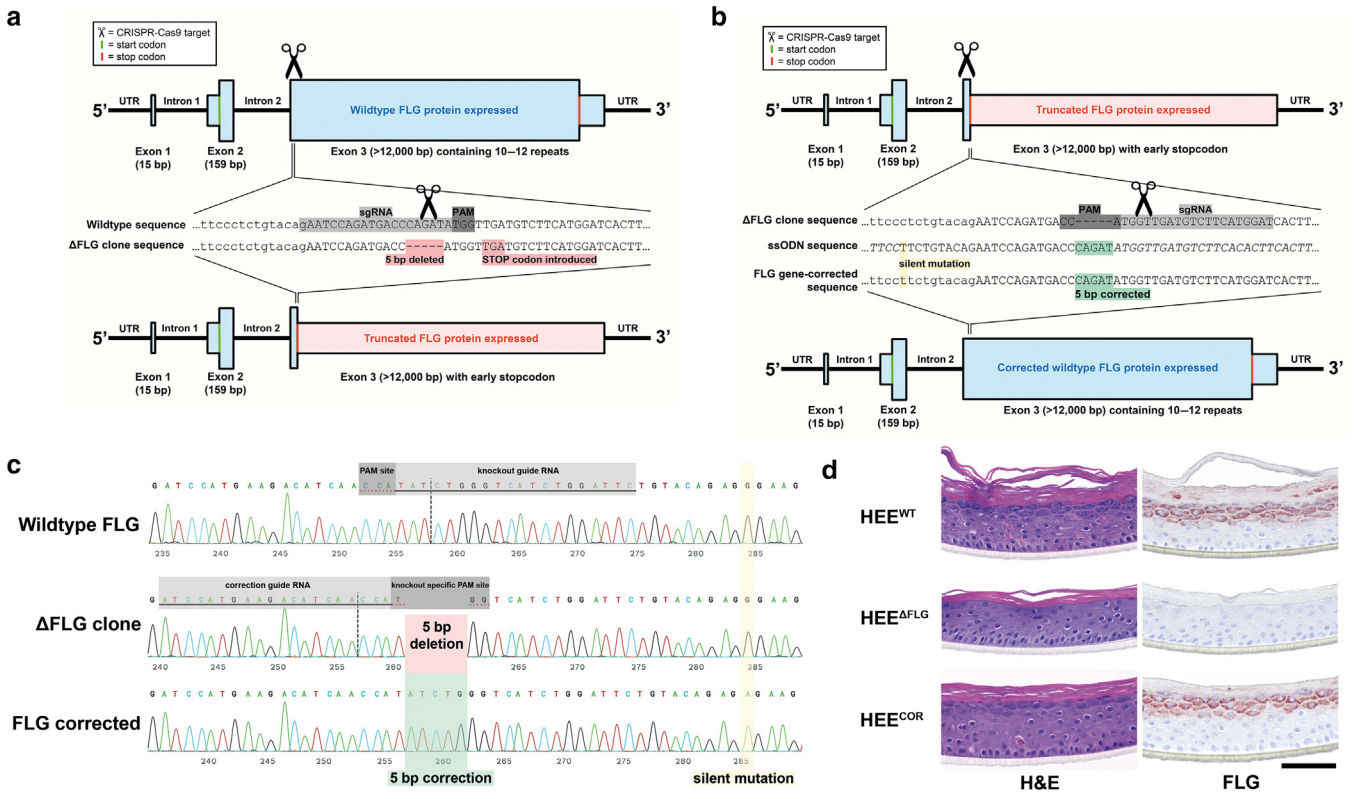

Figure 2. Validation of FLG expression in ΔFLG and FLG-corrected cultures. (**a, b**) Schematic representation of the genomic changes in the ΔFLG clone and FLG-corrected clone, respectively. (**c**) PCR-amplified *FLG* sequence (reverse complement sequence depicted) indicates a 5 bp deletion (c.152del5) leading to a predicted p.P51HfsX3 frameshift mutation with an early stop codon in the ΔFLG clone and restoration of the 5 bp deletion in the FLG-corrected clone. (**d**) FLG protein expression is lost in $HEE^{\Delta FLG}$, accompanied by a complete loss of keratohyalin granules, whereas FLG expression and keratohyalin granules are fully restored in HEE^{COR}. Bar = 100 μm. HEE, human epidermal equivalent; UTR, untranslated region.

FLG expression is essential for epidermal barrier function

To study whether the differential gene and protein expression patterns in $HEE^{\Delta FLG}$ would have functional consequences, we first performed two qualitative microscopic analyses by small molecule permeation of lucifer yellow (for gross stratum corneum defects) and EZ-link sulfo-NHS-LC-biotin (for qualitative tight junction functioning [Chen et al., 1997; Furuse et al., 2002]). No apparent changes in the permeation of the dyes were observed (Figure 4a). Similar to what is known from in vivo studies in patients with known FLG deficiency (Flohr et al., 2010), the quantitative barrier analyses by electrical impedance spectroscopy (Figure 4b) and transepidermal water loss (Figure 4c) showed a significant impairment of barrier function (lower electrical impedance spectroscopy and higher transepidermal water loss) upon FLG deficiency ($HEE^{\Delta FLG}$), whereas functional properties were regained upon *FLG* gene correction (HEE^{COR}).

DISCUSSION

In this study, we showcase straightforward ribonucleoprotein-based genomic editing in immortalized N/TERT KCs without the use of plasmids or viral vectors that incorporate their genetic material. Because N/TERT-2G KCs can be expanded in clonal (dilution) series, there is no need for antibiotic or fluorescence-activated selection procedures, thereby CRISPR/Cas9 genome editing can be harnessed rather easily in many research programs and may revolutionize the investigative dermatology field. In reality, we observed that its implementation is rather slow on the basis of the number of publications using (immortalized) KCs compared with that of publications using any cell type (Smits et al., 2022). Therefore, we deem it important to showcase how to disrupt (and reinstate) the protein of interest in the immortalized N/TERT-2G KC cell line. Genome editing as we performed utilizes nonhomologous end joining, a repair mechanism that is completely stochastic and unpredictable but suitable to generate random insertions and deletions (Gallagher and Haber, 2018). For subsequent specific corrective editing, we successfully employed a homology-directed repair strategy by supplying a donor oligonucleotide carrying the desired gene-correcting DNA sequence. Given the highly intriguing—yet partly undefined—role of (pro-)FLG in skin barrier function and the remaining knowledge gap on the therapeutic targeting of FLG deficiency, we focused on the *FLG* gene in this proof-of-principle study by targeting its N-terminal domain leading to a full protein knockout.

The identification of *FLG* loss-of-function variants and copy number variations as genetic risk factors for AD (Barker et al., 2007; Brown et al., 2012; Palmer et al., 2006; Sandilands et al., 2007) underscores the importance of the epidermal compartment in the pathogenesis of complex immune-mediated diseases. Fundamental research into the role of pro-FLG in AD pathophysiology has primarily addressed the palette of contributing pro-FLG–degrading factors (de Veer

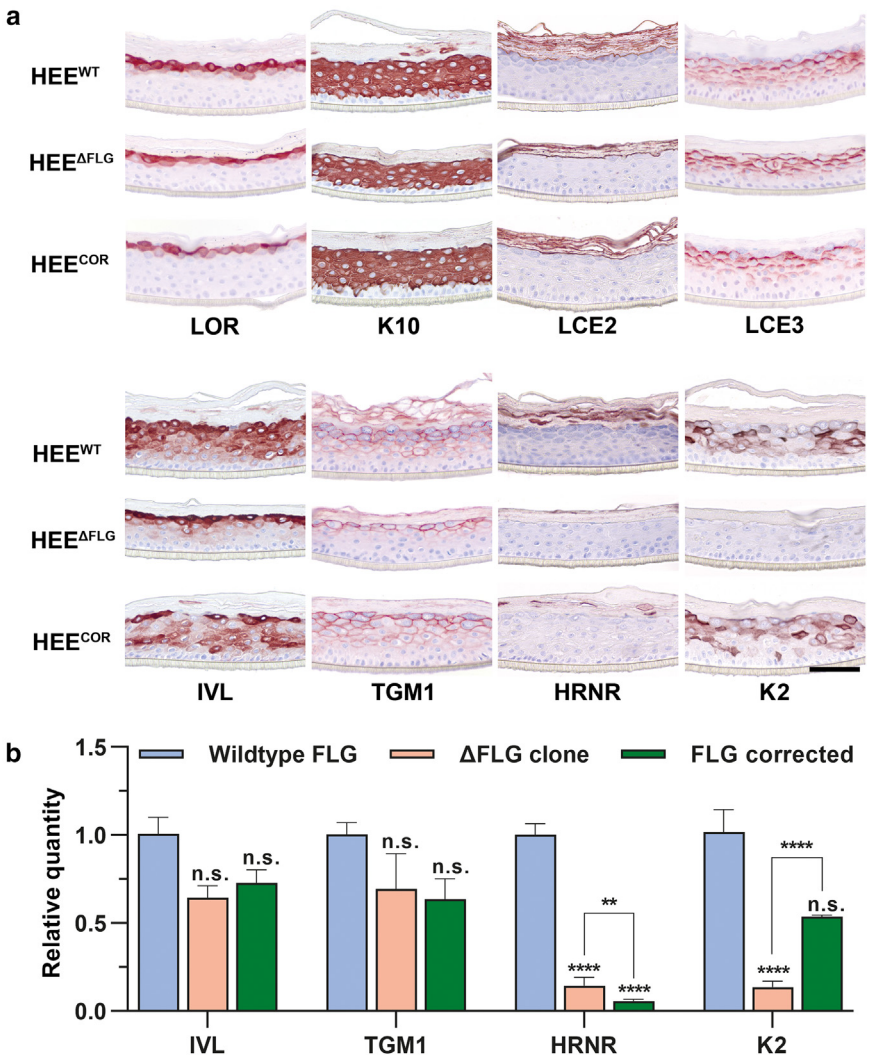

Figure 3. K2 and HRNR are completely abrogated as a result of FLG-knockout. (**a**) Immunohistochemical staining for several differentiation protein expressions shows similarities between FLG wild-type (HEE^{WT}), ΔFLG clone ($HEE^{\Delta FLG}$), and FLG-corrected clone (HEE^{COR}) (upper panel). Nevertheless, $HEE^{\Delta FLG}$ displays a downregulation of IVL and TGM1, whereas K2 and HRNR expressions were completely lost. Upon FLG correction (HEE^{COR}), the expression of IVL, TGM1, and K2 was completely restored, whereas HRNR expression was partly restored (lower panel). (**b**) Quantitative PCR to analyze gene expression of differentially expressed proteins shows minor downregulation of *IVL* and *TGM1* and major downregulation of *HRNR* and *K2* in the ΔFLG clone. FLG correction shows no effect on *IVL*, *TGM1*, and *HRNR* expression, whereas *K2* expression is partially restored to control levels. n = 3 HEE cultures. $^{**}P < 0.01$ and $^{****}P < 0.0001$. Bar = 100 μm. HEE, human epidermal equivalent; HRNR, hornerin; IVL, involucrin; K2, keratin 2; n.s., nonsignificant; TGM1, transglutaminase 1.

et al., 2014; Ovaere et al., 2009), for example, skin-specific retroviral-like aspartic protease (Matsui et al., 2011), kallikrein-related peptidase 5 (Sakabe et al., 2013), MT-SP1 (List et al., 2003), and furin (Pearton et al., 2001). Further processing of FLG into NMFs can be attributed to proteases like caspase 14 (Hoste et al., 2011) and bleomycin hydrolase (Kamata et al., 2009). Whereas these studies on the breakdown and processing of pro-FLG into FLG monomers and amino acids and crosslinking to keratin intermediate filaments are abundant, studies on the N-terminal domains of pro-FLG and their functions are scarce.

Analysis of the structure and functional domains of pro-FLG showed that the N-terminal fragment of pro-FLG contains a nuclear localization signal enabling its translocation to the nucleus before the onset of terminal differentiation (Aho et al., 2012; Ishida-Yamamoto et al., 1998; Presland et al., 1997; Zhang et al., 2002). It has been hypothesized that the translocated N-terminal fragment promotes KC denucleation in apoptotic terminally differentiating KCs (Ishida-Yamamoto et al., 1998). In addition, the pro-FLG N-terminal fragment potentially regulates epidermal differentiation genes, as suggested before (Pearton et al., 2002), and may halt KC proliferation upon overexpression of the pro-FLG N-terminus (Aho et al., 2012). Similar to our experiments on ΔFLG clonal KCs, small interfering RNA–mediated knockdown studies also do not report on altered proliferation rates or epidermal thickness due to FLG loss (Mildner et al., 2010).

The truncated pro-FLG that is expressed in AD and ichthyosis vulgaris disease–associated genotypes (e.g., p.R501X, c.2282del4, p.R2447X) still has an unaffected N-terminus that potentially can translocate to the nucleus. In fact, the most predominant variants in the *FLG* gene are situated downstream of the A and B domains, although truncating sequence variants have also been found in the A domain (van Leersum et al., 2020). Whether these rare early variants are also associated with atopic disease is not clear. Early truncating variants, for example, the deletion of 17 nucleotides (c.411del17 [Oji et al., 2009]), are located downstream of the nuclear localization signal, suggesting a great importance of the A and (partial) B domain of pro-FLG. Moreover, this would imply that expression of truncated pro-FLG and downstream proteolytic processing of the N-terminal part of pro-FLG—at least including the nuclear localization signal—might be intact in all of the known disease-associated *FLG* genotypes. The ΔFLG KCs reported in this paper express an incomplete N-terminal fragment that harbors only part of the pro-FLG A domain (50 amino acids) and

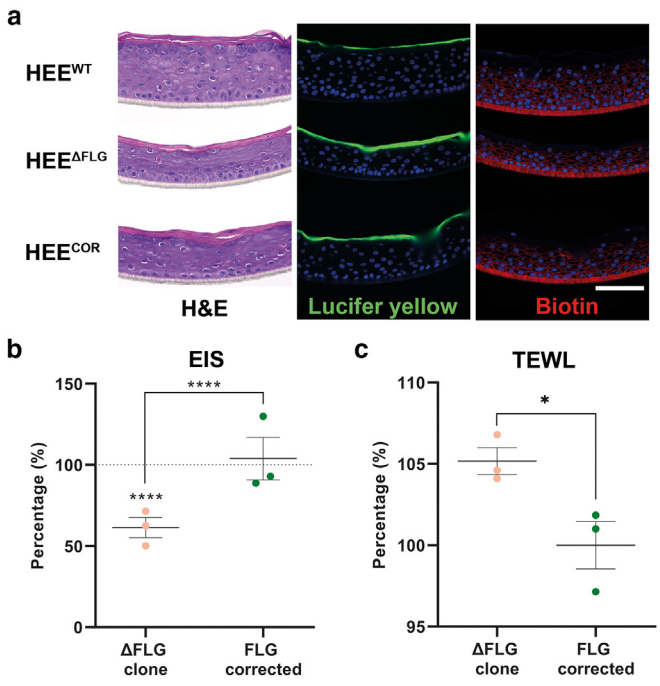

Figure 4. Knockout of FLG is accompanied by subtle changes in functional barrier properties that improve upon FLG reinstation. (**a**) Lucifer yellow and biotin permeation assays do not display aberrant functional barrier properties of the 3D epidermal equivalent cultures. Nevertheless, (**b**) EIS and (**c**) TEWL analysis show significant improvement of barrier properties in FLG-corrected keratinocytes compared with that in the ΔFLG clone. n = 3 HEE. $^{*}P < 0.05$ and $^{****}P < 0.0001$. Bar = 100 μm. 3D, three-dimensional; EIS, electrical impedance spectroscopy; HEE, human epidermal equivalent; TEWL, transepidermal water loss.

completely lacks the B domain. The B domain contains a putative nuclear localization signal. These ΔFLG KCs could leverage a new cellular model to study the biological function of FLG in the epidermis when comparing these cells with similarly created cells harboring disease-associated *FLG* genotypes. This will be the subject of further research.

Our data indicate that the loss of pro-FLG expression results in altered differentiation gene expression, for example, HRNR and involucrin, are both downregulated, as was previously shown by *FLG*-knockdown experiments (Pendaries et al., 2014). Interestingly, these genes are commonly downregulated in AD (Wu et al., 2009), and their expression is reduced upon stimulation with T helper 2 cytokines IL-4 and IL-13 in vitro (Kim et al., 2008; Pellerin et al., 2013; van den Bogaard et al., 2013). Furthermore, parallel downregulation of HRNR and FLG has been described (Pellerin et al., 2013), which is in line with the data presented in this paper. The concomitant downregulation in AD may thus not be due to merely the T helper 2 cytokine milieu, as previously suggested (Pellerin et al., 2013), but also result from loss-of-function variants in *FLG*. In addition, we identified other important proteins to be largely downregulated in ΔFLG KCs. Of particular interest is *K2*, the disease-causing gene in superficial epidermolytic ichthyosis (or ichthyosis bullosa of Siemens) (Kremer et al., 1994; Steijlen et al., 1994), a congenital skin disease characterized by dry skin and barrier loss (Traupe et al., 1986) and recently found to be differentially expressed in patients with vesicular hand eczema (Voorberg et al., 2021). We hypothesize that the pro-FLG N-terminal fragment can fulfill a regulatory function in the epidermis. This would explain the observed loss of specific epidermal proteins, such as K2, under knockout conditions, whereas its loss is not reported in any of the well-studied *FLG* loss-of-function variants that still express the N-terminal pro-FLG fragment. Besides having a potential regulatory function in the epidermis, it was reported that FLG might function as a structural anchoring protein in the terminally differentiating KCs (Candi et al., 2005; Eckhart et al., 2013). The loss of FLG then implies that other differentiation proteins, for example, involucrin, are less stabilized and consequently more prone to degradation by proteasomal machinery. Although this does not explain sustained downregulation even after correction of the ΔFLG genotype, as seen for HRNR.

Microscopic qualitative analysis of lucifer yellow and biotin permeation did not indicate gross functional barrier disturbance in HEEs from ΔFLG KCs, which is in line with our previous findings on patient-derived *FLG* null KCs (Niehues et al., 2017). Nevertheless, the quantitative and presumably more sensitive barrier measurements we now performed (electrical impedance spectroscopy and transepidermal water loss) indicate that the loss of FLG does affect barrier properties of HEEs, which is reversed by reinstating FLG expression. Whether this is directly or indirectly linked to the proposed scaffolding properties of FLG (Gutowska-Owsiak et al., 2018) requires further investigation, likewise the comparison of the ΔFLG-associated barrier impairment to patient-derived HEEs. Furthermore, additional analyses could be focused on the regulation of tight junction–associated genes and proteins (Winge et al., 2011) and on the organization of structural intercellular lipid lamellae, which are considered important for functional barrier properties of the stratum corneum (Riethmuller et al., 2015).

For the clinical translation of our findings, the next steps are aimed at the reproduction of common *FLG* variants (e.g., p.R501X, c.2282del4, and p.R2447X) in N/TERT-2G immortalized KCs to allow for a better comparison of genotype–phenotype differences in organotypic skin models within an otherwise identical genetic background. The subsequent exposure to disease–associated inflammatory mediators or environmental factors enables the characterization of gene–environment interactions that drive multifactorial diseases, such as AD. In this study, we present the key technology and translational tools for generating unique human KCs to create epidermal models with defined *FLG* variants, in which future integrative multiomics analysis can elucidate the modes of action through which pro-FLG controls terminal differentiation and potentially finding new therapeutic options for AD and ichthyosis vulgaris to restore epidermal homeostasis.

MATERIALS AND METHODS

Culturing and freezing of human N/TERT-2G KCs

Human N/TERT KC cell line N/TERT-2G, purchased from J. Rheinwald laboratory (Harvard Medical School, Boston, MA), was cultured in Epilife medium (MEPI500CA, Thermo Fisher Scientific, Waltham, MA), complemented with human KC growth supplement (S0015, Thermo Fisher Scientific) and 1% penicillin/streptomycin

(P4333, Sigma-Aldrich, St. Louis, MO). On generation of the different clonal N/TERT-2G KC cell lines, they were frozen in liquid nitrogen. In short, N/TERT-2G KCs were detached from culture plastic using 0.25% trypsin/EDTA (25200-072, Thermo Fisher Scientific). A similar amount of DMEM containing fetal calf serum was used to stop trypsin/EDTA activity, and the cells were washed twice with Dulbecco's PBS (BE17-512F, Lonza Bioscience, Basel, Switzerland) before resuspension in Epilife medium. After cell counting, the cell suspension was diluted one on one with DMEM containing 20% fetal calf serum and 20% DMSO and slowly frozen in MrFrosty freezing containers (Thermo Fisher Scientific) before moving them to liquid nitrogen storage.

N/TERT-2G HEE generation

Epidermal equivalents were generated as previously described (Smits et al., 2017), with minor adjustments. Briefly, inert Nunc cell culture inserts (141002, Thermo Fisher Scientific) were coated with rat tail collagen (100 μg/ml, BD Biosciences, Bedford, MA) at 4 °C for 1 hour. A total of 1.5×10^5 N/TERT-2G KCs were seeded on the transwells in 150 μl Epilife medium (Thermo Fisher Scientific) supplemented with 1% penicillin/streptomycin (Sigma-Aldrich) in a 24-wells format. After 48 hours, cultures were switched to a mixture of CnT-PR-3D medium (CELLnTEC, Bern, Switzerland) and DMEM medium (60:40 [v/v]) without penicillin/streptomycin for 24 hours and then cultured at the air–liquid interface for an additional 10 days. The culture medium was refreshed every other day until harvesting on day 10 of the air-exposed phase.

sgRNA design, single-strand donor oligonucleotide, and synthetic Cas9

Synthetic sgRNAs to knockout *FLG* gene and purified Edit-R Cas9 nuclease protein (nuclear localization signal, number CAS11200) were obtained from Synthego (Menlo Park, CA) and IDT Technologies (Coralville, IA), respectively. Custom synthetic Alt-R sgRNAs and single-strand donor oligonucleotide to correct FLG expression were ordered from IDT Technologies. See Supplementary Table S4 for details on the sgRNAs and single-strand donor oligonucleotide used.

Electroporation of ribonucleoprotein complexes and analysis of editing efficiency

N/TERT-2G KCs were electroporated using the NEON transfection system 10 μl kit (Thermo Fisher Scientific) (Evrard et al., 2021). Per electroporation condition, synthetic sgRNA (300 ng) and Cas9 (1.5 μg) were incubated with 5 μl resuspension buffer R for 20 minutes before adding 1×10^5 N/TERT-2G KCs. After mixing the cell suspension, the cells were electroporated using 1 pulse of 1,700 V for a duration of 20 ms before immediate seeding in a six-well plate. DNA was isolated using the QIAamp DNA blood mini kit (51106, Qiagen, Hilden, Germany) according to the manufacturer's instructions after reaching approximately 50% confluency, and CRISPR/Cas9-induced editing efficiency was analyzed by PCR and separation of amplicon on 2% agarose gel containing 1:10,000 GelRed nucleic acid gel stain (41003, Biotium, Fremont, CA). Amplicons were purified by MinElute Gel extraction kit (28606, Qiagen) as per the manufacturer's instructions and Sanger sequenced to assess editing efficiency. Sanger-sequencing reads were analyzed using the Inference of CRISPR Edits webtool (ice.synthego.com, version 2, Synthego). See Supplementary Table S5 for details on the PCR primers used.

Generation of clonal ΔFLG N/TERT KCs

ΔFLG N/TERT-2G KC cell pool and FLG gene–corrected N/TERT-2G KC cell pool were diluted to one cell per 100 μl Epilife medium and seeded into 6× 96-well plates and 100 μl cell suspension per well and allowed to grow for 1 week before refreshing the medium. After another week of culture, cells were passaged, as described earlier, into 24-well plates, 6-well plates, T25 flasks, and T75 flasks subsequently before freezing into liquid nitrogen. Cell clonality was assessed by Sanger sequencing and analyzing genomic DNA at the targeted *FLG* locus with the help of the Inference of CRISPR Edits webtool (ice.synthego.com, version 2, Synthego).

Additional methods are available as Supplementary Materials and Methods.

Data availability statement

No large genomic datasets were generated during this study.

ORCIDs

Jos P. H. Smits: http://orcid.org/0000-0003-0915-8624
Noa J. M. van den Brink: http://orcid.org/0000-0002-0826-4823
Luca D. Meesters: http://orcid.org/0000-0002-2554-7761
Hadia Hamdaoui: http://orcid.org/0000-0001-5020-8051
Hanna Niehues: http://orcid.org/0000-0002-6954-6955
Patrick A. M. Jansen: http://orcid.org/0000-0002-7894-2140
Ivonne M. J. J. van Vlijmen-Willems: http://orcid.org/0000-0002-3522-2573
Diana Rodijk-Olthuis: http://orcid.org/0000-0002-7752-6209
Céline Evrard: http://orcid.org/0000-0002-7450-0759
Yves Poumay: http://orcid.org/0000-0001-5200-3367
Michel van Geel: http://orcid.org/0000-0002-0273-8020
Wiljan J. A. J. Hendriks: http://orcid.org/0000-0001-9481-8281
Joost Schalkwijk: https://orcid.org/0000-0002-1308-1319
Patrick L. J. M. Zeeuwen: http://orcid.org/0000-0002-6878-2438
Ellen H. van den Bogaard: http://orcid.org/0000-0003-4846-0287

CONFLICT OF INTEREST

The authors state no conflict of interest. This publication reflects only the author's view and the JU is not responsible for any use that may be made of the information it contains.

ACKNOWLEDGMENTS

This work was supported by a LEO foundation grant LF18068 (PZ and EB), PAST4FUTURE grant LSHM20043-HSGF (EB), and Innovative Medicines Initiative 2 Joint Undertaking (JU) grant under grant agreement (No. 821511, EB). The JU receives support from the European Union's Horizon 2020 research and innovation program and EFPIA. The Graphical abstract was created with Biorender.com.

AUTHOR CONTRIBUTIONS

Conceptualization: JPHS, WJAJH, JS, PLJMZ, EHVDB; Data Curation: JPHS; Formal Analysis: JPHS; Funding Acquisition: EHVDB, PLJMZ, JS; Investigation: JPHS, NJMVDB, LDM, HH, HN, PLJMJ, IMJJVVW, DRO, MVG; Methodology: JPHS, NJMVDB, HH, CE, YP, WJAJH; Project Administration: EHVDB; Software: JPHS; Supervision: PZ, EHVDB; Validation: JPHS; Visualization: JPHS; Writing – Original Draft Preparation: JPHS; Writing – Review and Editing: JPHS, HN, JS, EHVDB, PLJMZ

SUPPLEMENTARY MATERIAL

Supplementary material is linked to the online version of the paper at www.jidonline.org, and at https://doi.org/10.1016/j.jid.2023.02.021.

REFERENCES

Aho S, Harding CR, Lee JM, Meldrum H, Bosko CA. Regulatory role for the profilaggrin N-terminal domain in epidermal homeostasis. J Invest Dermatol 2012;132:2376–85.

Barker JN, Palmer CN, Zhao Y, Liao H, Hull PR, Lee SP, et al. Null mutations in the filaggrin gene (FLG) determine major susceptibility to early-onset atopic dermatitis that persists into adulthood. J Invest Dermatol 2007;127:564–7.

Brown SJ, Kroboth K, Sandilands A, Campbell LE, Pohler E, Kezic S, et al. Intragenic copy number variation within filaggrin contributes to the risk of atopic dermatitis with a dose-dependent effect. J Invest Dermatol 2012;132:98–104.

Candi E, Schmidt R, Melino G. The cornified envelope: a model of cell death in the skin. Nat Rev Mol Cell Biol 2005;6:328–40.

Chen Y, Merzdorf C, Paul DL, Goodenough DA. COOH terminus of occludin is required for tight junction barrier function in early Xenopus embryos. J Cell Biol 1997;138:891–9.

Concordet JP, Haeussler M. CRISPOR: intuitive guide selection for CRISPR/Cas9 genome editing experiments and screens. Nucleic Acids Res 2018;46:W242–5.

Cong L, Ran FA, Cox D, Lin S, Barretto R, Habib N, et al. Multiplex genome engineering using CRISPR/Cas systems. Science 2013;339:819–23.

de Veer SJ, Furio L, Harris JM, Hovnanian A. Proteases: common culprits in human skin disorders. Trends Mol Med 2014;20:166–78.

Dickson MA, Hahn WC, Ino Y, Ronfard V, Wu JY, Weinberg RA, et al. Human keratinocytes that express hTERT and also bypass a p16(INK4a)-enforced mechanism that limits life span become immortal yet retain normal growth and differentiation characteristics. Mol Cell Biol 2000;20:1436–47.

Eckhart L, Lippens S, Tschachler E, Declercq W. Cell death by cornification. Biochim Biophys Acta 2013;1833:3471–80.

Evrard C, Faway E, De Vuyst E, Svensek O, De Glas V, Bergerat D, et al. Deletion of TNFAIP6 gene in human keratinocytes demonstrates a role for TSG-6 to retain hyaluronan inside epidermis. JID Innov 2021;1:100054.

Flohr C, England K, Radulovic S, McLean WH, Campbel LE, Barker J, et al. Filaggrin loss-of-function mutations are associated with early-onset eczema, eczema severity and transepidermal water loss at 3 months of age. Br J Dermatol 2010;163:1333–6.

Furuse M, Hata M, Furuse K, Yoshida Y, Haratake A, Sugitani Y, et al. Claudin-based tight junctions are crucial for the mammalian epidermal barrier: a lesson from claudin-1-deficient mice. J Cell Biol 2002;156:1099–111.

Gallagher DN, Haber JE. Repair of a site-specific DNA cleavage: old-school lessons for Cas9-mediated gene editing. ACS Chem Biol 2018;13:397–405.

Gasiunas G, Barrangou R, Horvath P, Siksnys V. Cas9-crRNA ribonucleoprotein complex mediates specific DNA cleavage for adaptive immunity in bacteria. Proc Natl Acad Sci U S A 2012;109:E2579–86.

Gutowska-Owsiak D, de La Serna JB, Fritzsche M, Naeem A, Podobas EI, Leeming M, et al. Orchestrated control of filaggrin-actin scaffolds underpins cornification. Cell Death Dis 2018;9:412.

Horii I, Nakayama Y, Obata M, Tagami H. Stratum corneum hydration and amino acid content in xerotic skin. Br J Dermatol 1989;121:587–92.

Hoste E, Kemperman P, Devos M, Denecker G, Kezic S, Yau N, et al. Caspase-14 is required for filaggrin degradation to natural moisturizing factors in the skin. J Invest Dermatol 2011;131:2233–41.

Ishida-Yamamoto A, Takahashi H, Presland RB, Dale BA, Iizuka H. Translocation of profilaggrin N-terminal domain into keratinocyte nuclei with fragmented DNA in normal human skin and loricrin keratoderma. Lab Invest 1998;78:1245–53.

Jakasa I, Koster ES, Calkoen F, McLean WH, Campbell LE, Bos JD, et al. Skin barrier function in healthy subjects and patients with atopic dermatitis in relation to filaggrin loss-of-function mutations. J Invest Dermatol 2011;131:540–2.

Jinek M, Chylinski K, Fonfara I, Hauer M, Doudna JA, Charpentier E. A programmable dual-RNA-guided DNA endonuclease in adaptive bacterial immunity. Science 2012;337:816–21.

Kamata Y, Taniguchi A, Yamamoto M, Nomura J, Ishihara K, Takahara H, et al. Neutral cysteine protease bleomycin hydrolase is essential for the breakdown of deiminated filaggrin into amino acids. J Biol Chem 2009;284:12829–36.

Kawasaki H, Nagao K, Kubo A, Hata T, Shimizu A, Mizuno H, et al. Altered stratum corneum barrier and enhanced percutaneous immune responses in filaggrin-null mice. J Allergy Clin Immunol 2012;129:1538–46.e6.

Kezic S, Kemperman PM, Koster ES, de Jongh CM, Thio HB, Campbell LE, et al. Loss-of-function mutations in the filaggrin gene lead to reduced level of natural moisturizing factor in the stratum corneum. J Invest Dermatol 2008;128:2117–9.

Kim BE, Leung DY, Boguniewicz M, Howell MD. Loricrin and involucrin expression is down-regulated by Th2 cytokines through STAT-6. Clin Immunol 2008;126:332–7.

Kremer H, Zeeuwen P, McLean WH, Mariman EC, Lane EB, van de Kerkhof CM, et al. Ichthyosis bullosa of Siemens is caused by mutations in the keratin 2e gene. J Invest Dermatol 1994;103:286–9.

List K, Szabo R, Wertz PW, Segre J, Haudenschild CC, Kim SY, et al. Loss of proteolytically processed filaggrin caused by epidermal deletion of matriptase/MT-SP1. J Cell Biol 2003;163:901–10.

Mali P, Yang L, Esvelt KM, Aach J, Guell M, DiCarlo JE, et al. RNA-guided human genome engineering via Cas9. Science 2013;339:823–6.

Matsui T, Miyamoto K, Kubo A, Kawasaki H, Ebihara T, Hata K, et al. SASPase regulates stratum corneum hydration through profilaggrin-to-filaggrin processing. EMBO Mol Med 2011;3:320–33.

Mildner M, Jin J, Eckhart L, Kezic S, Gruber F, Barresi C, et al. Knockdown of filaggrin impairs diffusion barrier function and increases UV sensitivity in a human skin model. J Invest Dermatol 2010;130:2286–94.

Niehues H, Schalkwijk J, van Vlijmen-Willems IMJJ, Rodijk-Olthuis D, van Rossum MM, Wladykowski E, et al. Epidermal equivalents of filaggrin null keratinocytes do not show impaired skin barrier function. J Allergy Clin Immunol 2017;139:1979–81.e13.

Oji V, Seller N, Sandilands A, Gruber R, Gerss J, Hüffmeier U, et al. Ichthyosis vulgaris: novel FLG mutations in the German population and high presence of CD1a+ cells in the epidermis of the atopic subgroup. Br J Dermatol 2009;160:771–81.

Ovaere P, Lippens S, Vandenabeele P, Declercq W. The emerging roles of serine protease cascades in the epidermis. Trends Biochem Sci 2009;34:453–63.

Palmer CN, Irvine AD, Terron-Kwiatkowski A, Zhao Y, Liao H, Lee SP, et al. Common loss-of-function variants of the epidermal barrier protein filaggrin are a major predisposing factor for atopic dermatitis. Nat Genet 2006;38:441–6.

Pearton DJ, Dale BA, Presland RB. Functional analysis of the profilaggrin N-terminal peptide: identification of domains that regulate nuclear and cytoplasmic distribution. J Invest Dermatol 2002;119:661–9.

Pearton DJ, Nirunsuksiri W, Rehemtulla A, Lewis SP, Presland RB, Dale BA. Proprotein convertase expression and localization in epidermis: evidence for multiple roles and substrates. Exp Dermatol 2001;10:193–203.

Pellerin L, Henry J, Hsu CY, Balica S, Jean-Decoster C, Méchin MC, et al. Defects of filaggrin-like proteins in both lesional and nonlesional atopic skin. J Allergy Clin Immunol 2013;131:1094–102.

Pendaries V, Malaisse J, Pellerin L, Le Lamer M, Nachat R, Kezic S, et al. Knockdown of filaggrin in a three-dimensional reconstructed human epidermis impairs keratinocyte differentiation. J Invest Dermatol 2014;134:2938–46.

Presland RB, Kimball JR, Kautsky MB, Lewis SP, Lo CY, Dale BA. Evidence for specific proteolytic cleavage of the N-terminal domain of human profilaggrin during epidermal differentiation. J Invest Dermatol 1997;108:170–8.

Riethmuller C, McAleer MA, Koppes SA, Abdayem R, Franz J, Haftek M, et al. Filaggrin breakdown products determine corneocyte conformation in patients with atopic dermatitis. J Allergy Clin Immunol 2015;136:1573–80.e2.

Sakabe J, Yamamoto M, Hirakawa S, Motoyama A, Ohta I, Tatsuno K, et al. Kallikrein-related peptidase 5 functions in proteolytic processing of profilaggrin in cultured human keratinocytes. J Biol Chem 2013;288:17179–89.

Sandilands A, Terron-Kwiatkowski A, Hull PR, O'Regan GM, Clayton TH, Watson RM, et al. Comprehensive analysis of the gene encoding filaggrin uncovers prevalent and rare mutations in ichthyosis vulgaris and atopic eczema. Nat Genet 2007;39:650–4.

Scott IR, Harding CR. Filaggrin breakdown to water binding compounds during development of the rat stratum corneum is controlled by the water activity of the environment. Dev Biol 1986;115:84–92.

Shi H, Smits JPH, van den Bogaard EH, Brewer MG. Research techniques made simple: delivery of the CRISPR/Cas9 components into epidermal cells. J Invest Dermatol 2021;141:1375–81.e1.

Smith FJ, Irvine AD, Terron-Kwiatkowski A, Sandilands A, Campbell LE, Zhao Y, et al. Loss-of-function mutations in the gene encoding filaggrin cause ichthyosis vulgaris. Nat Genet 2006;38:337–42.

Smits JPH, Meesters LD, Maste BGW, Zhou H, Zeeuwen PLJM, van den Bogaard EH. CRISPR-Cas9–based genomic engineering in keratinocytes: from technology to application. JID Innov 2022;2:100082.

Smits JPH, Niehues H, Rikken G, van Vlijmen-Willems IMJJ, van de Zande GWHJF, Zeeuwen PLJM, et al. Immortalized N/TERT keratinocytes as an alternative cell source in 3D human epidermal models. Sci Rep 2017;7:11838.

Steijlen PM, Kremer H, Vakilzadeh F, Happle R, Lavrijsen AP, Ropers HH, et al. Genetic linkage of the keratin type II gene cluster with ichthyosis bullosa of Siemens and with autosomal dominant ichthyosis exfoliativa. J Invest Dermatol 1994;103:282–5.

Traupe H, Kolde G, Hamm H, Happle R. Ichthyosis bullosa of Siemens: a unique type of epidermolytic hyperkeratosis. J Am Acad Dermatol 1986;14:1000–5.

van den Bogaard EH, Bergboer JG, Vonk-Bergers M, van Vlijmen-Willems IM, Hato SV, van der Valk PG, et al. Coal tar induces AHR-dependent skin barrier repair in atopic dermatitis. J Clin Invest 2013;123:917–27.

van Leersum FS, Nagtzaam IF, van Oosterhoud CN, Ghesquiere SAI, Brandts RRHFJ, Gostyński A, et al. Improving the diagnostic yield for filaggrin: concealed mutations in the Dutch population. J Allergy Clin Immunol 2020;145:1704–6.e2.

Voorberg AN, Niehues H, Oosterhaven JAF, Romeijn GLE, van Vlijmen-Willems IMJJ, van Erp PEJ, et al. Vesicular hand eczema transcriptome analysis provides insights into its pathophysiology. Exp Dermatol 2021;30:1775–86.

Winge MC, Hoppe T, Berne B, Vahlquist A, Nordenskjöld M, Bradley M, et al. Filaggrin genotype determines functional and molecular alterations in skin of patients with atopic dermatitis and ichthyosis vulgaris. PLoS One 2011;6:e28254.

Wu Z, Meyer-Hoffert U, Reithmayer K, Paus R, Hansmann B, He Y, et al. Highly complex peptide aggregates of the S100 fused-type protein hornerin are present in human skin. J Invest Dermatol 2009;129:1446–58.

Zhang D, Karunaratne S, Kessler M, Mahony D, Rothnagel JA. Characterization of mouse profilaggrin: evidence for nuclear engulfment and translocation of the profilaggrin B-domain during epidermal differentiation. J Invest Dermatol 2002;119:905–12.

SUPPLEMENTARY MATERIALS AND METHODS

In silico search for potential off-target effects

CRISPOR (version 4.98) (Concordet and Haeussler, 2018) was used to search for potential off-target sites dependent on the *Streptococcus pyogenes*–derived Cas9 protospacer adjacent motif site (5′-NGG-3′), target genome (*Homo sapiens* GRCh38/hg38), and our specific single-guide RNA selection. The top five potential off-target sites, ranked on cutting frequency determination score (Doench et al., 2016), were amplified by PCR and analyzed by Sanger sequencing to assure that no off-target mutations occurred. See Supplementary Table S5 for details on the PCR primers used.

Protein sequence prediction

EMBOSS Transeq (https://www.ebi.ac.uk/Tools/st/emboss_transeq/), a webtool designed to predict the translation of mRNA sequence into protein amino acid sequence, was used with standard settings to predict the result of the DNA mutations generated (Rice et al., 2000).

Morphological and immunohistochemical analysis

Human epidermal equivalents (HEEs) were fixed in a 4% formalin solution for 4 hours and subsequently embedded in paraffin. A total of 6 μm sections were stained with H&E (Sigma-Aldrich, St. Louis, MO) or processed for immunohistochemical analysis. Sections were blocked for 15 minutes with 5% serum in PBS and subsequently incubated with primary antibody against the protein of interest for 1 hour at room temperature. Next, a 30-minute incubation step with biotinylated secondary antibody (Vector Laboratories, Burlingame, CA) was performed, followed by a 30-minute incubation with avidin-biotin complex (Vector laboratories). The peroxidase activity of 3-amino-9-ethylcarbazole was used to visualize the protein expression, and the sections were mounted using glycerol gelatin (Sigma-Aldrich). See Supplementary Table S6 for details on the primary antibodies used.

Transcriptional analysis

Total RNA was isolated using the Favorprep total tissue RNA kit (Favorgen Biotech, Tung, Taiwan), according to the manufacturer's instructions. cDNA was generated after DNase treatment and used for RT-qPCR by use of the MyiQ Single-Colour Real-Time Detection System (Bio-Rad Laboratories, Hercules, CA) for quantification with Sybr Green and melting curve analysis. Primers (Supplementary Table S7) were obtained from Biolegio (Nijmegen, The Netherlands) and Merck KGaA (Darmstadt, Germany). Target gene expression levels were normalized to the expression of human acidic *RPLP0*. The relative expression levels of all genes of interest were measured using the 2-ΔΔCT method (Livak and Schmittgen, 2001). Two-way ANOVA with Tukey's multiple comparison tests was performed on the ΔCT values to assess statistical significance.

Lucifer yellow dye penetration assay

To study the outside-instratum corneum barrier function, 20 μl Lucifer Yellow (1 mM, Sigma-Aldrich) was applied on top of the HEEs and was allowed to incubate for 60 minutes in the dark at room temperature. HEEs were fixed in buffered 4% formalin solution, embedded in paraffin, and sectioned. A total of 6 μm sections were deparaffinized and mounted with Fluoromount-G, containing DAPI (eBioscience San Diego, CA).

Biotin penetration assay

To study the inside-outstratum corneum barrier function, the HEEs were turned upside down, and 20 μl EZ-link sulfo-NHS-LC-biotin (3.3 mg/ml, Thermo Fisher Scientific, Waltham, MA) was applied on the bottom of the filters and allowed to incubate for 60 minutes at room temperature. HEEs were fixated in buffered 4% formalin solution, embedded in paraffin, and sectioned. A total of 6 μm sections were deparaffinized and incubated for 30 minutes in the dark, with 1:200 Alexa Fluor 594 streptavidin (Thermo Fisher Scientific) conjugate. The sections were mounted with Fluoromount-G containing DAPI.

Electrical impedance spectroscopy and transepidermal water loss

Whereas transepithelial electrical resistance measurements are suitable for detecting barrier properties related to tight junction presence and functionality, electrical impedance spectroscopy is more suitable for epidermal equivalent cultures because it is a composed measure of transepithelial electrical resistance and electrical capacity of the cell compartment. Electrical impedance spectroscopy was measured using the real-time impedance detector Locsense Artemis (Locsense, Enschede, The Netherlands) equipped with SmartSense lid for monitoring cells in conventional transwell plates containing inserts. After lowering day 10 air-exposed HEE cultures to the middle position of the culture plate, 500 μl of PBS was added on top, and 1,100 μl PBS was added beneath the transwell filter. After calibration, continuous impedance (Ω) was measured while sweeping frequency from 10 Hz to 100,000 Hz. Afterward, the measured impedance was corrected for blank impedance per electrode and corrected for culture insert size (0.47 cm^2), resulting in impedance per cm^2 values (Ω/cm^2). Subsequently, measured phase values along the same frequency reach were used to pinpoint the frequencies where the contribution of cellular capacity was relatively limited. Mean impedance per cm^2 at these three frequencies was used to calculate relative differences between conditions. Two-way ANOVA with Tukey's multiple comparison test was performed to assess statistical significance. Transepidermal water loss was measured after equilibration of the HEE cultures to room temperature using the Aquaflux AF200 (Biox, London, United Kingdom) on day 10 of the air-exposed phase of the HEE culture, as described before (Niehues et al., 2017). Unpaired parametric *t*-test was used to assess statistical significance.

SUPPLEMENTARY REFERENCES

Bergboer JG, Tjabringa GS, Kamsteeg M, van Vlijmen-Willems IM, Rodijk-Olthuis D, Jansen PA, et al. Psoriasis risk genes of the late cornified envelope-3 group are distinctly expressed compared with genes of other LCE groups. Am J Pathol 2011;178:1470–7.

Concordet JP, Haeussler M. CRISPOR: intuitive guide selection for CRISPR/Cas9 genome editing experiments and screens. Nucleic Acids Res 2018;46:W242–5.

Doench JG, Fusi N, Sullender M, Hegde M, Vaimberg EW, Donovan KF, et al. Optimized sgRNA design to maximize activity and minimize off-target effects of CRISPR-Cas9. Nat Biotechnol 2016;34:184–91.

Livak KJ, Schmittgen TD. Analysis of relative gene expression data using real-time quantitative PCR and the 2(-Delta Delta C(T)) Method. Methods 2001;25:402–8.

Niehues H, Schalkwijk J, van Vlijmen-Willems IMJJ, Rodijk-Olthuis D, van Rossum MM, Wladykowski E, et al. Epidermal equivalents of filaggrin null keratinocytes do not show impaired skin barrier function. J Allergy Clin Immunol 2017;139:1979–81.e13.

Rice P, Longden I, Bleasby A. EMBOSS: the European molecular biology open software suite. Trends Genet 2000;16:276–7.

van Duijnhoven JL, Schalkwijk J, Kranenborg MH, van Vlijmen-Willems IM, Groeneveld A, van Erp PE, et al. MON-150, a versatile monoclonal antibody against involucrin: characterization and applications. Arch Dermatol Res 1992;284:167–72.

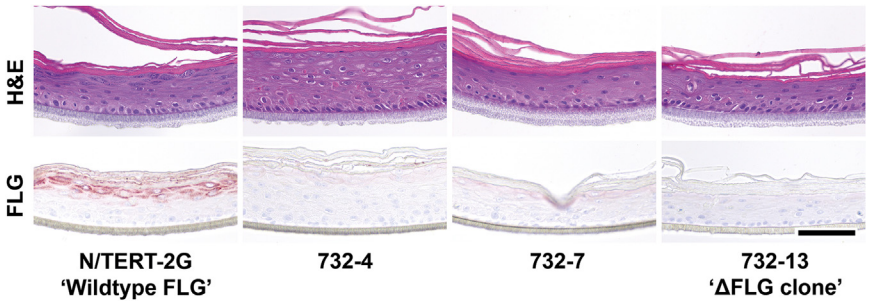

Supplementary Figure S1. Three ΔFLG N/TERT-2G clonal keratinocyte cell lines. After the clonal expansion of ΔFLG pool, ΔFLG clonal cells were isolated (732-4, 732-7, and 732-13). Clonal cells 732-13 were renamed to ΔFLG clone and used throughout the manuscript. In HEE culture, all of the ΔFLG clonal cell lines show an absence of keratohyalin granules and FLG expression, whereas epidermal thickness between clonal cell lines varies. Bar = 100 μm. HEE, human epidermal equivalent.

Supplementary Table S1. Genomic Information on Isolated Clonal N/TERT-2G Keratinocytes

Name in Manuscript	Cell Line	Zygosity	FLG Expression	Allele 1	Allele 2	Predicted FLG Protein
Wild-type FLG	N/TERT-2G keratinocytes	Homozygous	Yes	Wild type	Wild type	Wild type, 4,061 amino acids
ΔFLG clone, 732-13	ΔFLG N/TERT-2G keratinocytes	Homozygous	No	c.152_156del	c.152_156del	Truncated, 52 amino acids
732-4	ΔFLG N/TERT-2G keratinocytes	Heterozygous	No	c.148_158del	c.151_160del	Truncated, 50 amino acids and 60 amino acids
732-7	ΔFLG N/TERT-2G keratinocytes	Homozygous	No	c.153_154del	c.153_154del	Truncated, 53 amino acids
FLG corrected	FLG-corrected N/TERT-2G keratinocytes	Homozygous	Yes	c.139-11C>T	c.139-11C>T	Wild type, 4,061 amino acids

Supplementary Table S4. Sequences of the sgRNAs and ssODN

Target	Name	sgRNA Sequence (5′–3′)	PAM Site	Strand
FLG	FLG wild-type	GAATCCAGATGACCCAGATA	TGG	–
Δ*FLG*	ΔFLG clone	ATCCATGAAGACATCAACCA	TGG	+

Target	ssODN Name	ssODN Sequence
Δ*FLG*	FLG correction ssODN	AATTGGCTGATAAT GTGATTCTGTCTGATGCAGTCTC CCTCTGTGACTTCTCTCTGTACAGAAT CCAGATGACCCAGA TATGGTTGATGTCTTCATGGAT CACTTGGATATAGACCA CAACAAGAAAATTGAC TTCACTGAGTTTCTTCT

Abbreviations: sgRNA, single-guide RNA; ssODN, single-strand donor oligonucleotide; PAM, protospacer adjacent motif.

Supplementary Table S5. PCR Primer Sequences

Gene	Target Name	Forward Primer (5′–3′)	Reverse Primer (5′–3′)
FLG	FLG wild-type	TGGCTGATAATGTGATTCTGTC	CTGTTTCTCTTGGGCTCTTGG

Name	Off-target site	Forward primer (5′–3′)	Reverse primer (5′–3′)
KO_Off1	intergenic:PROM2-KCNIP3	TTGAGAAAGCTCAGGCACAC	CACTCAGGCTAGAAGCGATG
KO_Off2	intergenic:MIR873-LINC01242	CTCCAGCCAACATCAAGAAA	TTTCCAAAGGGAATTGATCC
KO_Off3	intron:ELAVL2	GGACAGACATCTGCATTCATTC	TTACCAGATTGCGTCCTGTG
KO_Off4	intergenic:GMNC-OSTN	AGAAGCAGGCTGACACCTTT	CCCAGTGATGAGGAATGGAT
KO_Off5	intergenic:Y_RNA-RP11-112L7.1	CTGTGGTTTGGTCCATTCAG	GGGAGGTCTTGTCCAGTGAT
Cor_Off1	intron:ZC3H13	CTTCTGACGCTTCATTTCCA	AACCCAACTTCCAAACAACC
Cor_Off2	intron:LINC00375	GCCAAGGTATTCAAAAGATGG	ACAACAAAGCCTCCCTGAAT
Cor_Off3	intergenic:AC090573.1-RP11-65D17.1	CGCTCCTGCAACTTCAGTAA	AGATGGCTTTGGGGAGTATG
Cor_Off4	intron:SLC16A9	TCCCACAAACATTCCATGAG	CATCTGTGAAGGCAGGCTAA
Cor_Off5	intergenic:RP11-574O16.1-AC010887.1	GAGCCACAGAGCCTTCTTCT	AGAGCTGGGATTTGAGCCTA

Supplementary Table S6. Antibodies Used for Immunohistochemistry

Antibody; Clone	Manufacturer	Dilution
FLG; 1957R	LifeSpan BioSciences, Seattle, WA (catalog number LS-C751132)	1:200
LOR; polyclonal	Abcam, Cambridge, United Kingdom (catalog number ab85679)	1:3,000
K10; DE-K10	Progen Biotechnik GmbH	1:100
LCE2; #74	Bergboer et al., 2011	1:10,000
LCE3; clone 7	Abmart, Berkeley Heights, NJ	1:5,000
IVL; Mon150	Van Duijnhoven et al., 1992	1:20
TGM1; A-5	Santa Cruz Biotechnology, Dallas, TX (catalog number sc-365821)	1:100
HRNR; polyclonal	Sigma-Aldrich (catalog number HPA031469)	1:500
K2; Ks2.342.7.4	Progen Biotechnik GmbH, Heidelberg, Germany (catalog number 65191)	1:200

Abbreviations: HRNR, hornerin; IVL, involucrin; K, keratin; LCE, late cornified envelope; LOR, loricrin; TGM1, transglutaminase 1.

Supplementary Table S7. Quantitative PCR Primer Sequences

Gene	Target Name	Forward Primer (5′–3′)	Reverse Primer (5′–3′)
hARP	Human acidic ribosomal phosphoprotein P0	CACCATTGAAATCCTGAGTGATGT	TGACCAGCCCAAAGGAGAAG
IVL	Involucrin	ACTTATTTCGGGTCCGCTAGGT	GAGACATGTAGAGGGACAGAGTCAAG
TGM1	Transglutaminase 1	CCCCCGCAATGAGATCTACA	ATCCTCATGGTCCACGTACACA
HRNR	Hornerin	TACAAGGCGTCATCACTGTCATC	ATCTGGATCGTTTGGATTCTTCAG
K2	Keratin 2	CGCCACCTACCGCAAACT	GAAATGGTGCTGCTTGTCACA

Abbreviations: HRNR, hornerin; IVL, involucrin; K2, keratin 2; TGM1, transglutaminase 1.